Towards a Hybrid Architecture by Introducing Coherent Pluggable Transceivers in IP-Optical Core Networks with Optical Cross-Connects

Filippos Christou
Institute of Communication Networks and Computer Engineering (IKR)
University of Stuttgart
Stuttgart, Germany
filippos.christou@ikr.uni-stuttgart.de

Tobias Enderle
Institute of Communication Networks and Computer Engineering (IKR)
University of Stuttgart
Stuttgart, Germany
tobias.enderle@ikr.uni-stuttgart.de

Arthur Witt
Institute of Communication Networks and Computer Engineering (IKR)
University of Stuttgart
Stuttgart, Germany
arthur.witt@ikr.uni-stuttgart.de

***Abstract*—During the previous years, there has been a big technological advancement in Digital Signal Processing (DSP) and coherent pluggable optics, which enabled a considerable increase in the data rate and a step towards economical packet-optical integration, respectively. This caused the network operators to start wondering whether an architectural change should take place in their infrastructure. Coherent Pluggable Transceivers (CPTs), already being a success story for Data Center Interconnect (DCI), have grown to be used not only in metro networks but, as of recently, also in some parts of the core. The latter constitutes a major use case for the Multi-Source Agreement (MSA) OpenZR+. As many network operators can have good reasons to stick with the traditional standalone transponder equipment, this paper explores a hybrid solution combining CPTs and transponders to fully exploit the advantages of the two technologies. More specifically, we balance the trade-off between using cheaper pluggable modules directly on the IP router and powerful standalone flexible transponders with a gray interface. Although the integration of colored optics in the router was already proposed about a decade ago with Cisco's IPoD-WDM, we find that this time it is more appealing in terms of power consumption, module size, and equipment cost. Furthermore, we look closer at a collapsed packet-optical integrated architecture of Hop-by-Hop lightpath connections as opposed to a multilayer one, which also uses Optical Cross-Connects (OXCs). We show that a hybrid solution using both architectures yields the best results for improving network metrics and minimizing hardware costs. We contribute an Integer Linear Program (ILP) to solve the dimensioning problem for realistic countrywide topologies.**

***Index Terms*—Coherent pluggable transceivers, Hybrid architecture, Integer linear program, Network dimensioning**

I. Introduction

For decades, telecommunication networks have faced increasing traffic demands, and they will continue to do so in the foreseeable future. Today, transporting all this traffic without coherent optical transmission is hard to imagine. The market for optical transmission equipment is highly competitive. Network vendors are constantly improving their transponders to achieve higher signal reaches and larger capacities using sophisticated modulation schemes like Probabilistic Constellation Shaping (PCS), advanced Forward Error Correction (FEC), multi-carrier super-channels, and higher baud rates. In the following, we refer to this class of transponders as Coherent Elastic Transponders (CETs). While the evolution of CETs is important for transport networks of large telecommunication providers, coherent optics also found their way into the Data Center (DC) ecosystem during the last years. Inside the DC, traffic volumes have been increasing even stronger than in traditional transport networks, and the interconnection of such DCs now requires coherent optics as well. However, in contrast to the traditional telecommunication providers' approach of using top-notch, proprietary CETs, DC operators tend to focus on simplicity, cost efficiency, and interoperability. As a result, the Optical Internetworking Forum (OIF) released the 400ZR Implementation Agreement (IA), a de facto standard for a Coherent Pluggable Transceiver (CPT) for $400\,\mathrm{Gbps}$ Ethernet-based transmission. Allowing only $400\,\mathrm{Gbps}$ and no other data rates at a reach of about $120\,\mathrm{km}$, 400ZR transceivers are less powerful and less flexible than CETs. However, less flexibility means easier handling, and since 400ZR is an IA, transceivers of one vendor are interoperable with those of other vendors, which provides advantages in scalability, disaggregation, and cost efficiency. Additionally, 400ZR transceivers benefit from the growing integration of both electrical and optical components, which allows networking equipment to be built much smaller and much more power-efficient than in the past. As a result, 400ZR transceivers come in the QSFP-DD form factor and can be plugged into the router or switch ports directly. This eliminates the need for separate optics shelves and gray connections required by traditional transponder-based setups.

Inspired by the success of 400ZR, the OpenZR+ Multi-Source Agreement (MSA) was developed [1]. A ZR+ is another CPT that supports different modulation formats, several data rates and boosts signal reach with a standardized FEC. With that, it can be considered a viable alternative to traditional transponder-based setups in metro or even core networks of telecommunication providers. The principle idea is not new.

This work has been performed in the framework of the CELTIC-NEXT EUREKA project AI-NET-ANTILLAS (Project ID C2019/3-3), and it is partly funded by the German BMBF (Project ID 16KIS1312). The authors alone are responsible for the content of the paper.

More than a decade ago, Cisco developed the IP over DWDM (IPoDWDM) technology with the goal of integrating optics into the router. However, the technology did not gain traction because IPoDWDM line cards were expensive and occupied many precious router slots. Furthermore, the strict separation among telecommunication providers between IP and optics departments made the integration difficult. Nowadays, the separation of departments appears to be less strict, and the cost and space characteristics of OpenZR+ are better than those of IPoDWDM. The first providers already use OpenZR+ transceivers in their core networks [2], but the majority seems still hesitant.

In this work, we compare different scenarios to decide whether OpenZR+ is a sensible choice for a provider's network. More importantly, we find the best way to combine CPTs and CETs in the considered problem instances by developing an Integer Linear Program (ILP). On top of that, we examine the influence of a Hop-by-Hop (HbH) architecture by reducing the number of Optical Cross-Connects (OXCs) in the network and discover how much that can be beneficial. We realize that incorporating a combination of all these paradigms is the most cost-efficient yet powerful enough architecture case for the network dimensioning problem.

The following section introduces literature related to our study. In Section III, we put the problem statement in concrete terms. Section IV presents the assumed architecture model. Section V contains a detailed description of the ILP we used for network dimensioning. Section VI introduces the different scenarios we compared, and the corresponding results are discussed in Section VII. Finally, we conclude the paper in Section VIII.

II. Related Work

In [3] the British Telecommunications Group analyzed different network scenarios where CPTs are used. They also consider traditional Reconfigurable Optical Add-Drop Multiplexer (ROADM) networks with CETs to allow direct connections between source and destination nodes as a reference solution. An interesting scenario is a mixed network architecture, where $400\,\mathrm{Gbps}$ CPTs are used on links where the distance allows it, and traditional 400G CETs are used for the longer ones. The evaluation of an 8-year network planning scenario with a $30\,\%$ traffic increase per year shows that the mixed architecture will be the most cost-efficient in the long run.

The authors of [4] introduced an ILP to compare CPTs with CETs under the consideration of line-side protection or optical restoration mechanisms. Line-side protection requires the provisioning of a protection path with the same channel settings as the working path. CETs can be used here very efficiently as only a few additional transponders are needed. CPTs will have to reduce the transmission rate to reach the longer distances for the protection paths, which will increase the number of modules significantly. In optical restoration, where spectral resources can be shared for working and protection paths, the number of CPT interfaces is greatly reduced.

IP-optical architectures for metro, regional, and long-haul networks are compared in [5]. The authors identify that CETs are suitable for long-haul networks as they provide the best spectral efficiency and largest optical reach. For metro or regional networks, CPTs directly plugged in at router ports are preferable.

The most recent publication in this field [6] considers three network architectures: (a) CPTs in a HbH network, (b) CPTs with an OXC at every node, and (c) CETs with rates of up to $800\,\mathrm{Gbps}$ and an OXC at every node. Their ILP-based evaluation for the US Coronet and a pan-India topology significantly reduces required equipment like transmission modules and gray interfaces if the flexible and high-performance CETs are used.

III. Objective

Traditionally, the IP-optical core networks are equipped with high-end CETs that provide increased flexibility in adaptive modulation schemes and utilization of optical bandwidth. Nowadays, inter-DC connections are often realized with CPTs to offer an exclusive and direct connection between the data centers. These connections are integrated into the traditional core networks, which naturally leads to a network architecture with various transmission modules. Consequently, we want to discuss if a mixture of CETs and CPTs can be used to increase the efficiency of core networks while keeping low costs. Further, various network architectures will be studied. First, a traditional multilayer network that allows optical bypassing. Second, a flat HbH network. Third, a hybrid architecture where only some nodes are equipped with an OXC. This architecture aims mainly to reduce hardware costs and still provide the opportunity for bypassing.

Those issues can be seen as network planning and dimensioning problems that are highly interesting for network operators who want to keep their equipment up to date. Therefore, we want to introduce a method to optimize and evaluate network configurations with various transmission module technologies based on an ILP formulation. We also overview several metrics, such as router port utilization, spectrum allocation, signal regenerations, latency, energy consumption, and hardware costs. These metrics are evaluated for both cases of electrical grooming being allowed or not.

IV. Architecture Model

This section will describe some architectural choices and assumptions fundamental to carrying out the study as described in the previous chapter.

A. Network and Network Nodes

Let us consider a network described by a unidirectional graph $G(V, E)$ with V the set of vertices and E the set of edges. For each $e \in E$, we signify the distance of the fiber used on this link as $length(e)$. The set $U = \{(u, v) \in V \times V : u \neq v\}$ contains all node pairs. Each vertex in the graph corresponds to a node in the network, either a router or a router and an OXC. Each router contains several line cards, where each line card $l \in L$ has a tuple of properties (n_l, r_l, c_l) being the port density, the maximum port rate, and the cost of the line card, respectively. Having a set of line cards L and a specific line card l, we signify the line card with the next lower port rate in the set as $l_{\text{low}} = lower(L, l)$. Table I shows the available line cards L.

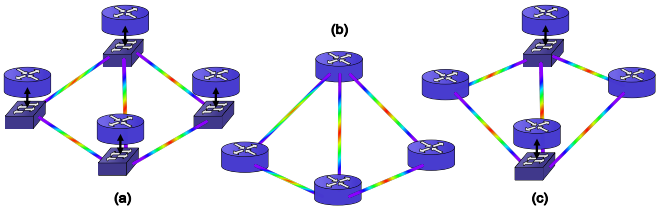

Fig. 1. The (a) Multilayer, (b) HbH, and (c) hybrid architectures.

The values are based on the predictions of [7], meaning that costs are normalized to the cost of a 10 Gbps transponder in the year 2012. Moreover, the line cards are grouped into line card chassis, with each one having a constant capacity of $N_{\text{lcc}} = 16$ line card slots and a price of 4.7 cost units. An OXC is realized using a colorless, directionless, contentionless (CDC) ROADM and serves to bypass the optical signals towards neighboring nodes without having to undergo Optical-Electrical-Optical (O-E-O) conversion. The percentage of OXCs in the network signifies the number of nodes having an OXC, and it can range from $0\,\%$ being a full *HbH* architecture to $100\,\%$ being a full *multilayer* architecture. Of great interest in this study will be all the values in between, and such architecture will be characterized as *hybrid*. Figure 1 depicts the network architectures mentioned above, while Figure 2 illustrates the block architecture of a multilayer 2-degree node as considered in this study. More specifically, a router contains multiple line card chassis, and each one contains up to 16 line cards. Each line card includes a variable amount of ports. The router ports are connected to a transponder through a gray interface or they directly hold a pluggable. Then the signal is fed to the add/drop layer of the OXC. The internal representation of the ROADM is taken from [7] and will later be valuable for the overall cost calculations.

B. Network Properties

We further consider a static demand matrix D with $D_{s,d}$ being the traffic requested from node s to node d for $(s,d) \in U$. Demands are being served using the lightpaths in P, where $P_{i,j}$ with $(i,j) \in U$ includes all candidate lightpaths connecting node i with j. Each lightpath $p \in P$ has a particular length of $length(p)$, starts at a node $start(p)$, terminates at a node $end(p)$, and travels through all the in-between nodes in the optical domain. The combination of all adjacent optical channels is given by C, with C_x being all the adjacent channels that reserve x continuous slots. Assuming FlexGrid with a slot width granularity of 12.5 GHz in the C-Band, we define the enumeration S, which contains all frequency slot indices ranging from 1 to 320. For example, C_4 would be the set of all combinations of four contiguous slots from 1 to 320, i.e. $\{1,2,3,4\},\{2,3,4,5\},\{3,4,5,6\},...,\{317,318,319,320\}$.

An optical transmission module is capable, due to its elasticity, of a set of transmission modes $t \in T$ being described by a tuple $(d_t, r_t, b_t, c_t, t_t)$, where:

- d_t is the optical reach in kilometers, assuming Erbium-Doped Fiber Amplifier (EDFA) amplification in every span of $80\,\text{km}$.
- r_t is the data rate.
- b_t is the number of frequency slots occupied as a multiple of $12.5\,\text{GHz}$.
- c_t is the cost of the module.
- t_t is the module type, either a CPT or a CET.

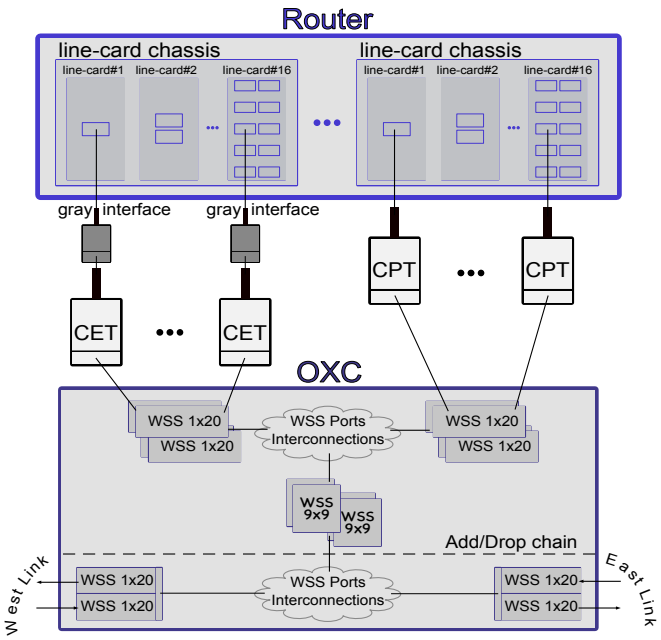

Fig. 2. The node architecture. The OXC is designed according to [7].

We narrowed these values down to Table II. Table IIa shows the properties of the OpenZR+ modules [1], while Table IIb and Table IIc show the transponder properties. The Table IIb assumes somewhat conservative values, while IIc considers more advanced technology and thus more powerful transponders with greater optical reach. This increase comes at the price of more bandwidth use. The reason for using two tables for the transponder properties is to demonstrate the influence of relatively weak versus powerful transponders as well as to demonstrate the flexibility of parametrization of the optimization ILP model. The values were derived from publications like [8], [4], from GNPy [9], and through some valuable feedback from industry partners to confirm their plausibility as products in the market. We generalized the cost of a CPT to be $40\,\%$ of the CET [3], thus setting them to 8 and 20 cost units, respectively.

TABLE I
PROPERTIES OF THE LINE CARDS.

Line cards L		
n_l (ports)	r_l port rate (Gbps)	c_l (cost units)
10	100	26.72
2	400	29.36
1	1000	31.99

C. Grooming and No-Grooming

Finally, we distinguish between two operating modes: the *grooming* and *no-grooming* modes. Electrical grooming is a

TABLE II
PROPERTIES OF THE OPTICAL TRANSMISSION MODULES

(a) Pluggable modules

CPT		
r_t (Gbps)	d_t (km)	b_t ($\times$ 12.5 GHz)
400	480	6
300	1600	6
200	2880	6
100	5840	4

(b) Transponder modules (conservative)

CET *conservative*		
r_t (Gbps)	d_t (km)	b_t ($\times$ 12.5 GHz)
800	160	8
700	200	8
600	240	6
500	480	6
400	880	6
300	2080	6
200	6120	6
100	9260	4

(c) Transponder modules (advanced)

CET *advanced*		
r_t (Gbps)	d_t (km)	b_t ($\times$ 12.5 GHz)
800	400	10
700	700	10
600	1200	8
500	2800	8
400	4400	8
300	5080	8

technique that serves to increase the spectrum utilization in the network by combining different optical signals into the same one. For this to happen, all the optical signals of interest must be converted to electrical signals and then be modulated together into the same optical channel. For example, when different lightpaths pass through the same links, network efficiency might benefit if these optical signals are grouped into a single lightpath. Such network benefits become less obvious for networks leveraging the FlexGrid or PCS technology, as each optical signal can theoretically have a precisely customized optical channel. Also, grooming techniques might increase the complexity of the path-finding algorithm involved or even yield increased hardware usage if not parametrized correctly. For these reasons, we include these two modes and measure the influence of electrical grooming in our scenarios.

V. METHODOLOGY

Following, we will present the procedure used to solve the resource allocation problem in optical networks, considering the architecture of the previous chapter. More precisely, given a network graph G, some resources like transmission modes T, line cards L, and optical channels C, the task is to derive the optimal resource allocation for a static traffic matrix D. Optimality is measured against the costs of the resources used as presented in Section IV. This is a network dimensioning problem; hence there is no resource limitation and traffic blocking. However, no overdimensioning is performed since that would not change the results of a comparative study like this one. The comparison will be between a HbH, a multilayer, or a hybrid network architecture and configurations using only CPTs, only CETs, or both. All these cases are treated by feeding in different inputs to an ILP, as described next.

A. ILP

As already mentioned, the primary task of the ILP is to determine the hardware resources to serve all demand pairs in the network. Different hardware presents different properties, which the ILP needs to consider to produce a cost-efficient configuration successfully.

The ILP is inspired from [8] while also incorporating modifications to support our specific scenario. Following, we present the complete ILP formulation and highlight the main differences from its predecessor. We will show two versions, one with electrical grooming and one without. First, we will describe the ILP input, variables, and constraints for the grooming case, and later we will point out the differences for the no-grooming version.

1) Input: This subsection will describe the model's parameters, which are treated as constants by the ILP. We form B as the set of all spectrum slot requirements b_t for $t \in T$. The candidate lightpaths P are collected using the k-shortest paths between all node pairs $(i, j) \in U$ to populate $P_{i,j}$.

The costs of the hardware resources used, play the role of the objective function coefficients. More specifically, we use:

- c_t being the cost of a module operating at transmission mode t.
- c_l being the cost of a line card l.
- c_{lcc} being the cost of a line card chassis.
- c_φ being the cost of an end-to-end fiber.
- $c_{\varphi\text{km}}$ being the cost of a fiber per kilometer.

Precise values of these costs are found in Section IV. We set c_φ to 100 cost units per fiber and $c_{\varphi\text{km}}$ to 0.5 cost units per fiber kilometer.

2) Variables: Following, we present the variables of the ILP system:

- $f_{s,d}^{i,j} \in \mathbb{R}_{\geq 0}$ $((s,d),(i,j) \in U)$ represents the traffic flow from source node s to destination node d using a lightpath from i to j.
- $x_{p,t} \in \mathbb{Z}_{\geq 0}$ $(p \in P, t \in T)$ is the number of deployed lightpaths p using transmission mode t. To have a valid lightpath-transmission mode pair, the optical reach of t needs to support the distance covered by the lightpath p.
- $u_{p,c} \in \mathbb{Z}_{\geq 0}$ $(p \in P, c \in C)$ is the number of deployed lightpaths p using channel c.
- $z_{v,l} \in \mathbb{Z}_{\geq 0}$ $(v \in V, l \in L)$ is the number of line cards of type l at node v. To use a transmission mode t in a line card, the port rate must be supported ($r_l \geq r_t$).
- $h_v \in \mathbb{Z}_{\geq 0}$ $(v \in V)$ is the number of line card chassis at node v.
- $\phi_e \in \mathbb{Z}_{>0}$ $(e \in E)$ is the number of fibers at edge e.

To get the number of line cards l per node, we need to create two more variables to represent an internal state:

- $\hat{z}_{v,l} \in \mathbb{Z}_{\geq 0}$ $(v \in V, l \in L)$ represents the line card l type ports that can be used at node v in order to serve the deployed lightpaths crossing this node.

- $\hat{\hat{z}}_{v,l} \in \mathbb{Z}_{\geq 0}$ $(v \in V, l \in L)$ signifies the requested number of ports at node v that can be allocated either with a line card of type l or any lower rate one.

3) Constraints and Objective Function: Following, we present the constraints:

$$\sum_{i \in V \setminus \{v\}} f_{s,d}^{i,v} - \sum_{j \in V \setminus \{v\}} f_{s,d}^{v,j} = \begin{cases} -D_{s,d}, & \text{if } v = s \\ +D_{s,d}, & \text{if } v = d \\ 0, & \text{if } v \neq s, d \end{cases} \quad (1)$$
$$\forall (s,d) \in U, v \in V$$

$$\sum_{(s,d) \in U} f_{s,d}^{i,j} \leq \sum_{p \in P_{i,j}, t \in T} r_t \cdot x_{p,t} \qquad \forall (i,j) \in U \quad (2)$$

$$\sum_{p \in P_{i,j}, t \in T | length(p) > d_t} x_{p,t} = 0 \qquad \forall (i,j) \in U \quad (3)$$

$$\sum_{t \in T | b_t = b} x_{p,t} = \sum_{c \in C_b} u_{p,c} \qquad \forall (p,b) \in P \times B \quad (4)$$

$$\sum_{c \in C, p \in P | s \in c \wedge e \in p} u_{p,c} \leq \phi_e \qquad \forall (e,s) \in E \times S \quad (5)$$

$$\hat{z}_{v,l} = \sum_{p \in P, t \in T | (start(p) = v \vee end(p) = v) \wedge r_l \geq r_t} x_{p,t} \qquad \forall (v,l) \in V \times L \quad (6)$$

$$\hat{\hat{z}}_{v,l} = \begin{cases} \hat{z}_{v,l} - \hat{z}_{v,l_{\text{low}}}, & \text{if } l_{\text{low}} = lower(L,l) \\ \hat{z}_{v,l}, & \text{if } \nexists lower(L,l) \end{cases} \quad (7)$$
$$\forall (v,l) \in V \times L$$

$$\sum_{l \in L | r_l \geq r_{\widehat{l}}} z_{v,l} \cdot n_l \geq \sum_{l \in L | r_l \geq r_{\widehat{l}}} \hat{\hat{z}}_{v,l} \qquad \forall (v, \widehat{l}) \in V \times L \quad (8)$$

$$h_v \geq \sum_{l \in L} z_{v,l} / N_{\text{lcc}} \qquad \forall v \in V \quad (9)$$

Constraint (1) holds the flow constraints. Each node can be either a traffic generator ($v = s$), a traffic sink ($v = d$), or a mediator, which will forward the traffic ($v \neq s, d$). The demands are being routed because of (2). This inequality obliges every flow to be served using a combination of a lightpath and a transmission mode. Equality (3) excludes such invalid combinations because of optical reach limitations. Later in (4), the specific super-channels are being chosen. The equation serves both the spectrum contiguity and continuity constraints. Inequality (5) handles the allocation of optical fibers. If the same super-channel is allocated more than once along a lightpath p, then more fibers need to be used. Equalities (6) and (7) constitute an internal state to precisely calculate the number of line cards needed. (8) takes over the final allocation of ports in terms of line cards. (9) reserves the line card chassis needed by accumulating the line cards in groups of N_{lcc}.

The objective function to be minimized is

$$\sum_{p \in P, t \in T} c_t \cdot x_{p,t} + \sum_{v \in V, l \in L} c_l \cdot z_{v,l} + \sum_{v \in V} c_{\text{lcc}} \cdot h_v + \sum_{e \in E} (c_\varphi + length(e) \cdot c_{\varphi \text{km}}) \cdot \phi_e. \quad (10)$$

The optimization target solely depends on the hardware equipment cost and not on network efficiency metrics. However, this ILP model implicitly works towards improving such network metrics since better network metrics lead to less equipment needed and vice versa. We will introduce some of these network metrics in Section VII.

4) Grooming restricted version: For the ILP version where grooming is not allowed, it is enough to substitute the variable x_{pt} with the following

- $x_{s,d}^{p,t} \in \mathbb{Z}_{\geq 0}$ $(p \in P, t \in T)$ is the number of deployed lightpaths p using transmission mode t for the flow between node s and node d.

Subsequently, we will need to substitute all constraints involving x_{pt} with the expression $\sum_{(s,d) \in U} x_{p,t}^{s,d}$ except for constraint number (2), for which we must not in order to keep track of single end-to-end flow allocations. Thus, constraint (2) becomes

$$f_{s,d}^{i,j} \leq \sum_{p \in P_{i,j}, t \in T} r_t \cdot x_{p,t}^{i,j} \qquad \forall (i,j) \in U, (s,d) \in U \quad (11)$$

These substitutions lead to a significant increase in the number of constraints, thus requiring more memory resources.

VI. Scenario

This chapter will present a concrete description of our use cases. We also introduce the specific parameters of our model. Finally, we will go through the simulation setup and some implementation details.

A. Network Parameters

As described in Section IV, there are several input parameters to be decided. Some of them are fixed, while others vary to observe their influence.

1) Fixed Input Parameters: After a series of simulations, the below parameters were chosen as fixed for the present study. The resource costs are kept constant to the values introduced in Section IV. The k-shortest path to calculate the set of candidate lightpaths P is fixed to $k = 2$. Each link has 320 available frequency slots. Finally, the static traffic matrix is left unchanged throughout all the simulations. The matrix D was artificially generated using a deterministic negative exponential relationship with respect to the node pair distance. Figure 3 shows the demand matrix on the left blue axis as considered for the US topology with a maximum demand value of $900\,\text{Gbps}$, a minimum of $50\,\text{Gbps}$, and the red dashed line shows the average demand value across all nodes pairs to $130\,\text{Gbps}$. The reader can see the node pair distances on the right orange axis.

2) Varying Input Parameters: To showcase the impact of some of the model inputs, we carried out a parametric sweep across all the combinations of the following parameters:

- *TopologyType* is either a US or a German topology. The two networks are shown in Figure 4. The topologies and node coordinates were retrieved from [10].
- *OXCPercentage* (OXCP) incorporates the percentage of OXCs in the network. The parameter values are increasing at a granularity of $10\,\%$, i. e. $0\,\%$, $10\,\%$, $20\,\%$, ..., $100\,\%$. The available OXCs are positioned in the network with

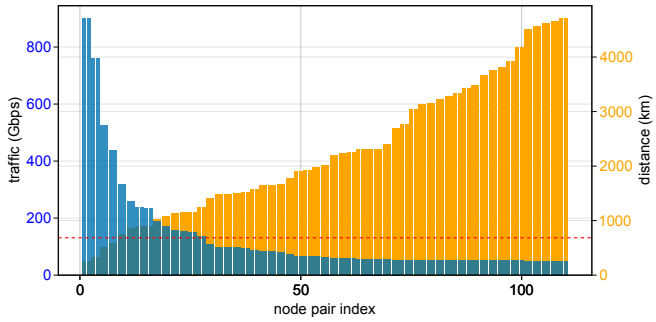

Fig. 3. The demand matrix D for the US network.

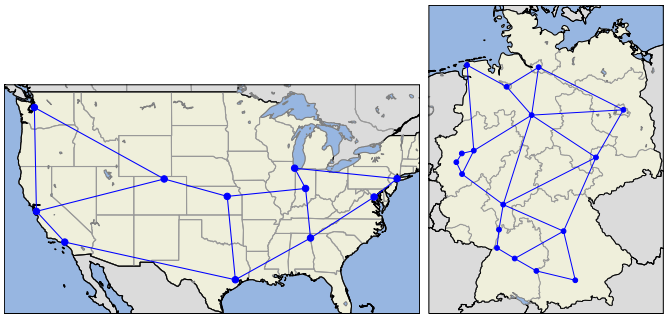

(a) US topology (avg. link length: 993 km)

(b) German topology (avg. link length: 143 km)

Fig. 4. The network topologies.

decreasing order at the nodes with higher betweenness centrality, using the link length as the shortest path metric.

- *ILPType* (ILPT) is the two operating modes and can be Groom or NoGroom.
- *TransType* (TransT) is the type of transmission modules used. Although the transmission properties tuples always remain the same as in Table II, we vary this parameter as follows:
  - *PurePluggables* (PP) contains only Table IIa.
  - *PureTransponders* (PT) contains only Table IIb.
  - *PureTranspondersBoosted* (PTB) contains Table IIb and Table IIc.
  - *Mixed* (M) contains Table IIa and Table IIb.
  - *MixedBoosted* (MB) contains all tuples in Table II.

The results of the parametric study are in Section VII.

B. Simulation Setup

The simulation, meta-analysis, and data visualization [11] were done using software written in Julia [12]. In particular, we used the JuMP framework [13] to model and formulate the ILP. The mathematical programming solver IBM CPLEX version 12.10 was used as a backend. We conducted our parameter study averaging over 4 seeds. For every seed, 8 threads were allocated leveraging the opportunistic mode of CPLEX, which enables the solver to aggressively search for the best solutions without caring for reproducibility. The relative tolerance on the ILP gap was set to $4\,\%$, and the time limit to stop any execution at $8\,\text{hours}$.

VII. Results

To interpret the impact of the variable parameters on network efficiency, we need to use some network metrics. Similar to [6], [5], we define the following:

- *Port usage* is the absolute number of router ports used.
- *Spectrum usage* is the total normalized spectrum allocated throughout the whole network.
- *Regenerations* are the total absolute amount of times a signal regenerates.
- *Latency* is the total normalized network latency as a summation of all end-to-end traffic requests. We assume the speed of light in the fiber to be $199\,861.213\,\text{km/sec}$.
- *Power consumption* is the total normalized power consumption of the network. We consider in line with [6], [14] CPTs of $15\,\text{Watt}$, CETs of $150\,\text{Watt}$, router ports of $36\,\text{Watt}$, and gray transceivers of $8\,\text{Watt}$.
- *Hardware Costs* are the total CAPEX costs of the network, as explained in Section IV. For the OXC, we consider a CDC, FlexGrid ROADM with the architecture of Figure 2, and the costs are calculated using the assumptions of [7].

The normalization happens with respect to the maximum value in each case, as shown later.

A. Port Usage

Figure 5 shows the port usage for both the US and the German topology. The available ports are the number of line cards times their port density, and the used ports are the allocated ports from the solver. The x-axis on the plots signifies the parameter in use, and the y-axis is the average of all simulations holding this parameter value steady. For example, we see that having $0\,\%$ OXCs yields the highest port usage for the US topology on average. The ILP tries to keep the used ports close to the available number in order not to pay for an extra line card.

In the same figure, we witness a behavior that will persist throughout most results. Namely, the network metric is rather bad when on $0\,\%$ OXCs and exponentially improves as we increase the OXC participation. However, the improvement rate decreases as the OXC percentage grows, and the metric converges to a particular number with negligible differences between the other high OXC values. We call it the *sufficient convergence point* where the knee of the curve is, and more OXCs will hardly make a difference (e. g., $50\,\%$ for the US and $30\,\%$ for Germany). So, unfortunately, there is not a panacea OXC percentage value for all networks, and finding this point depends very much on the topology in use. For example, the German topology is more interconnected than the US; thus, having fewer OXCs is fine.

Regarding the TransType parameter and due to the short distances in the German topology, we can observe that there is substantially no difference between using CPTs or CETs for the port usage metric. This is not the case for the US topology, where stronger transmission technology is needed to cross big distances. For this reason, the mixed Boosted case performs better than using only CPTs.

Also, it becomes obvious that no-grooming operation is generally much more resource-hungry than the grooming case.

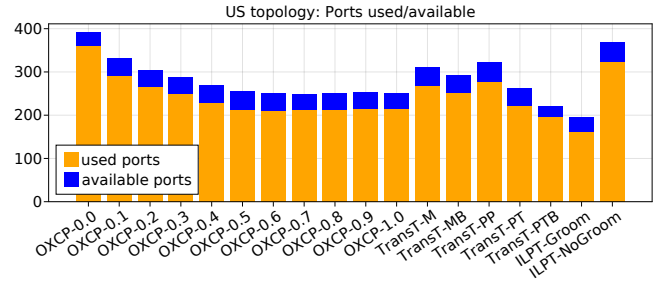

Fig. 5. Port usage parameter sweep.

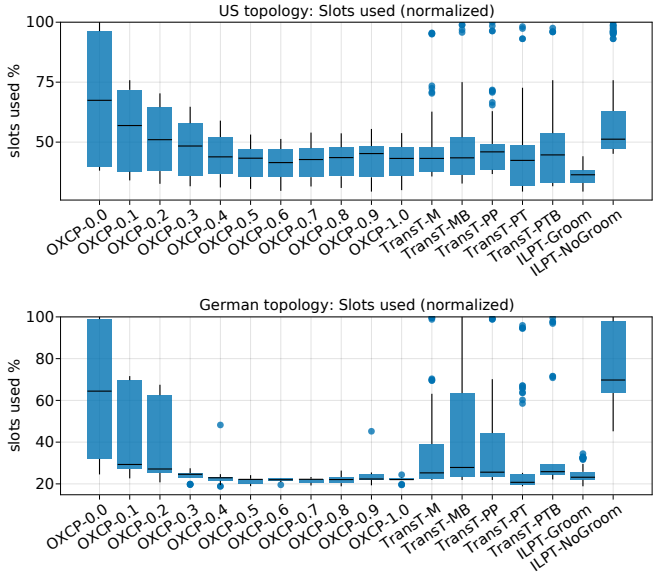

Fig. 6. Slot usage parameter sweep.

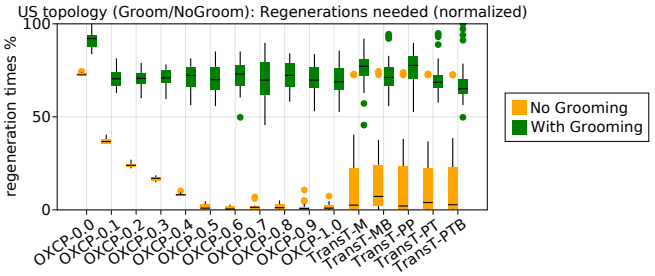

Fig. 7. Regeneration times parameter sweep.

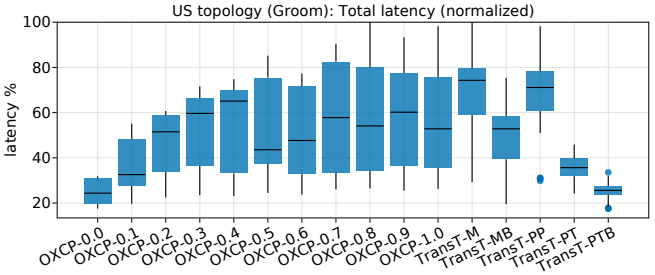

Fig. 8. Latency parameter sweep.

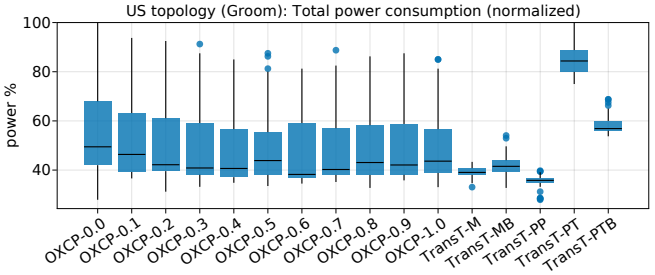

Fig. 9. Regeneration times parameter sweep.

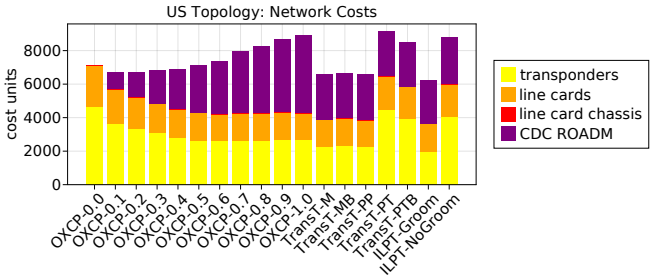

Fig. 10. Hardware costs parameter sweep.

B. Spectrum Usage

The spectrum allocation follows the same pattern as the port usage. This time, the box plots are presented in Figure 6. The crossbars span the Interquartile Range (IQR), with the midline marking the median, and the error bar whiskers span up to $1.5 \times$ IQR. Again, we witness that having $0\,\%$ OXCs yields the highest spectrum allocation. Hence, all other values will be normalized based on this maximum.

The slight increase of the powerful transponders (i. e. Boosted) compared to conventional transponders happens due to the increased problem complexity. The *MixedBoosted* and *PureTranspondersBoosted* are supersets of *Mixed* and *PureTransponders*, respectively, and naturally, they can only do better. The problem is that the more transponder tuples the ILP considers, the harder the problem becomes and the more variance in the results. The boxplots detect this uncertainty with a rather long crossbar and even longer whiskers. However, much of this variance comes from the no-grooming case due to its extreme behavior. This can be seen better in the next subchapter and Figure 7.

C. Regenerations

We will now continue only with the results of the US topology since the behavior of the two networks is similar. Observing Figure 7, we indeed conclude that the no-grooming

case introduces some more variance in our results for the different transmission modules. In addition, when grooming is not allowed, regeneration times are better minimized, approaching values close to zero. However, more OXCs are needed to reach the sufficient convergence point compared to the grooming case ($50\,\%$ against $10\,\%$ OXCs).

D. Latency

Another interesting impact is that lower latencies are achieved by decreasing the OXCs or preferring CETs over CPTs. Figure 8 shows exactly this for the US topology and grooming allowed. The major factor of these latencies is the propagation delay, as is commonly the case in core networks. When the OXC percentage is low, the ILP prefers to take the shortest path to route all demands. As the OXC percentage increases, more opportunities emerge to optimize the resource allocation by grooming and optically bypassing the signals using the second shortest paths, thus increasing the end-to-end delay. On the other hand, powerful transponders allow the solver to not commit to nearby regeneration points but route the traffic directly through the shortest path.

E. Power Consumption

Power consumption is a part of the network operator's OpEx costs. Figure 9 shows that a hybrid architecture consisting of both CPTs and CETs can have a power consumption very close to the one using only CPTs. We observe that the pure CET case is, in contrast, very power-hungry.

F. Hardware Costs

Figure 10 shows the overall network node costs of the US topology for the different parameters. The line card chassis are mostly constant to 1, so no multi-chassis routers are really needed with this traffic matrix. As the OXC percentage and the costs for ROADMs increase, the need for transponders decreases. Interestingly, overall costs balance around the same value 6500, up to $50\,\%$ OXCs. Regarding the transmission modules, once again, the mixed case is standing very close to the pure CPT case, which appears much more economical than the pure CET cases.

VIII. Conclusion

Overall in this paper, we discussed the problem of choosing between different core network architectures. We considered a multilayer architecture versus a HbH and networks using only CETs modules versus only CPTs. We showcased that the optimal behavior comes with a hybrid architecture for both cases, where we can have the best of two worlds. Unfortunately, finding the best architecture recipe is very much dependent on the network topology and the underlying resources, which were treated as problem parameters. We provided an ILP formulation to find this optimal point and examined it for several problem instances. We found that overly increasing the OXC coverage might saturate the network metrics, where no further win will be possible. This had more impact on a higher interconnected topology like the German network. Regarding the transmission modules, using both CETs and CPTs demonstrates costs close to the pure CPT case while at the same time approaching the better network metrics of the CETs. This was more apparent for large distance networks like the US backbone. The problem instance fed to the ILP can easily be adapted to any network operators' present or future perspectives.

References

[1] "White paper: OpenZR+ 400G Digital Coherent Optics for Multi-Haul," OpenZR+ Multi-Source Agreement, Tech. Rep., September 2020, Accessed on 28.03.2022. [Online]. Available: https://openzrplus.org/site/assets/files/1074/openzrplus_whitepaper_-_sept_29_2020_final.pdf

[2] Colt, "Colt takes network innovation to new heights with a 400G-capable Routed Optical Networking solution on its IQ Network," https://www.colt.net/resources/colt-takes-network-innovation-to-new-heights-with-a-400g-capable-routed-optical-networking-solution-on-its-iq-network/, Accessed on 28.03.2022.

[3] P. Wright, R. Davey, and A. Lord, "Cost Model Comparison of ZR/ZR+ Modules Against Traditional WDM Transponders for 400G IP/WDM Core Networks," in *2020 European Conference on Optical Communications (ECOC)*, 2020.

[4] A. Eira and J. Pedro, "On the Comparative Efficiency of Next-Generation Coherent Interfaces for Survivable Network Design," in *17th International Conference on the Design of Reliable Communication Networks (DRCN)*, 2021.

[5] S. Melle, T. Zami, O. Bertran-Pardo, and B. Lavigne, "Comparing IP-Optical Architectures & WDM Transport Technologies in Metro, Regional and Long-Haul Networks," in *2021 Optical Fiber Communications Conference and Exhibition (OFC)*, 2021.

[6] A. Gumaste, M. Sosa, H. Bock, and P. Kandappan, "Optimized IP-over-WDM core networks using ZR+ and flexible muxponders for 400 Gb/s and beyond," *Journal of Optical Communications and Networking*, vol. 14, no. 3, pp. 127–139, 2022.

[7] F. Rambach, B. Konrad, L. Dembeck, U. Gebhard, M. Gunkel, M. Quagliotti, L. Serra, and V. López, "A Multilayer Cost Model for Metro/Core Networks," *Journal of Optical Communications and Networking*, vol. 5, no. 3, pp. 210–225, 2013.

[8] P. Papanikolaou, K. Christodoulopoulos, and E. Varvarigos, "Multilayer flex-grid network planning," in *2015 International Conference on Optical Network Design and Modeling (ONDM)*, 2015, pp. 151–156.

[9] A. Ferrari, M. Filer, K. Balasubramanian, Y. Yin, E. Le Rouzic, J. Kundrát, G. Grammel, G. Galimberti, and V. Curri, "GNPy: an open source application for physical layer aware open optical networks," *Journal of Optical Communications and Networking*, vol. 12, no. 6, pp. C31–C40, 2020.

[10] S. Orlowski, M. Pióro, A. Tomaszewski, and R. Wessäly, "SNDlib 1.0–Survivable Network Design Library," in *3rd International Network Optimization Conference (INOC)*, 2007, http://sndlib.zib.de, Accessed on 28.03.2022.

[11] S. Danisch and J. Krumbiegel, "Makie.jl: Flexible high-performance data visualization for Julia," *Journal of Open Source Software*, vol. 6, no. 65, 2021.

[12] J. Bezanson, A. Edelman, S. Karpinski, and V. B. Shah, "Julia: A Fresh Approach to Numerical Computing," *SIAM review*, vol. 59, no. 1, pp. 65–98, 2017.

[13] I. Dunning, J. Huchette, and M. Lubin, "JuMP: A Modeling Language for Mathematical Optimization," *SIAM Review*, vol. 59, no. 2, pp. 295–320, 2017.

[14] W. Van Heddeghem and F. Idzikowski, "Equipment power consumption in optical multilayer networks – source data," Tech. Rep., January 2012.